Ultra-Wideband System for Museum Visitors Tracking: Towards the Integration of the Positioning System with the Vision Sensors

International Journal of Geo-Information

MDPI

Article

Ultra-Wideband System for Museum Visitors Tracking: Towards the Integration of the Positioning System with the Vision Sensors

Angeliki Makellaraki, Vincenzo Di Pietra, Paolo Dabove * and Milad Bagheri

Department of Environment, Land, and Infrastructure Engineering (DIATI), Politecnico di Torino, Corso Duca degli Abruzzi 24, 10129 Turin, Italy; angeliki.makellaraki@polito.it (A.M.); vincenzo.dipietra@polito.it (V.D.P.); milad.bagheri@polito.it (M.B.)

* Correspondence: paolo.dabove@polito.it

Abstract

Indoor positioning systems (IPSs) are increasingly applied in indoor settings where satellite-based GNSS signals are unavailable, including museums and other cultural heritage spaces. Within the META-MUSEUM project, we present a pilot study integrating an Ultra-Wideband (UWB) positioning system and an eye-tracking device to monitor and quantify visitor behavior in a real museum environment. The absence of common timestamps between the two systems, and the presence of UWB signal noise, have been the main challenges to address. A cross-correlation–based synchronization method was developed to align the two independent UWB and eye-tracking datasets. Data were collected from 100 visitors, of whom 7 different clusters were considered based on the characteristics of the visitors. The results demonstrate the system's feasibility and provide two complementary metrics, Normalized Engagement and Collective Engagement, which are used to quantify the duration and spatial distribution of visitor engagement at specific exhibits. This work establishes a scalable multi-sensor foundation by addressing practical deployment challenges under real-world conditions. These findings form the basis for the project's broader goal of linking spatial visitor behavior with neurophysiological responses, opening new possibilities for improving visitor engagement and supporting interactive cultural heritage experiences.

Keywords: indoor positioning; Ultra-Wideband; museum environment; cultural heritage; visitors tracking; sensors integration; eye-tracking

Academic Editors: Wolfgang Kainz and Eliseo Clementini

Received: 24 October 2025
Revised: 23 December 2025
Accepted: 2 January 2026
Published: 8 January 2026

1. Introduction

Cultural heritage plays a crucial role in shaping individual and collective identity, offering experiences that contribute not only to the acquisition of knowledge, but also to personal growth, social inclusion, and general well-being [1]. The ability to track visitors and understand their level of engagement within cultural spaces can help curators design more meaningful and engaging spaces. Several experimental studies have been carried out to investigate the visitor experience [2–4], with particular attention to emotional responses, levels of involvement with exhibits, and their spatial position.

Tracking objects and people in indoor spaces is quite different compared to outdoor environments. In the outdoors, the use of Global Navigation Satellite Systems (GNSS) is the main method of localization, providing reliable and accurate results. However, indoors, the situation is more complex due to the presence of various materials and obstacles that create non-line-of-sight (NLOS) conditions [5]. This limitation has led to the development and

implementation of several alternative radio technologies specifically designed to address the challenges of indoor environments [6–8], including Bluetooth Low Energy (BLE), Ultra-Wideband (UWB), Wi-Fi, acoustic systems, and infrared (IR) [9]. Drahanský et al. [10] reviewed several of these technologies and outlined their main advantages and limitations when applied to visitor monitoring in museum spaces. Among the available solutions, UWB has emerged as one of the most promising technologies, offering high accuracy and robustness in challenging indoor conditions, which motivates its use in the present work.

UWB already has practical application in different fields such as manufacturing, healthcare, agriculture, and warehouse management. It is a short-range radio communication system that offers precise localization and centimetric level of accuracy [11]. This high level of precision makes UWB a much more accurate option compared to alternatives like Bluetooth, which typically offers accuracy within 5 m, and Wi-Fi, which provides accuracy ranging from 5 to 15 m [12,13]. Unlike narrowband systems that are susceptible to signal overlap in multipath environments, UWB employs short-duration pulse modulation at the microsecond or nanosecond level, allowing it to effectively minimize interference from multiple signal paths [14]. Some additional advantages, include resistance to interference and jamming, and low power consumption, which make it particularly suitable for portable and battery-powered devices [15]. This technology has been the focus of various research activities. Di Pietra et al. [16] investigated a Pozyx® UWB-based positioning system for both indoor and outdoor pedestrian navigation scenarios, achieving a horizontal positioning accuracy of 35 cm. Similarly, D'Urso et al. [17] evaluated an UWB system in a laboratory environment designed to simulate a dairy barn, focusing on its performance in tracking static and dynamic positions. The system demonstrated an overall positioning accuracy of 50 cm under controlled conditions. Furthermore, Gnaś et al. [18] explored methods to improve UWB accuracy in complex environments such as warehouses. By integrating advanced algorithms like Machine Learning Enhanced Trilateration (MLET), their system achieved a mean positioning error of 11.31 cm.

This research is conducted within the framework of the European project META-MUSEUM, whose main goal is to understand how people respond to cultural heritage and how cultural experiences can help visitors develop emotional resilience and confidence. Rather than relying only on surveys, META-MUSEUM employs physiological sensors and brain activity monitoring to study visitor behavior inside museum rooms. In this context, having spatial information about where visitors are positioned adds significant value, as it makes it possible to determine whether specific responses are directly related to particular artifacts. Previous studies have examined visitor positioning and emotional responses, but most of them have relied on single-sensor methodologies or performed separate analyses [19]. In our study, we address the technical challenge of integrating positioning and eye-tracking sensors that do not share common timestamps. Specifically, we investigate the synchronization between spatial data from a low-cost UWB device and eye-tracking data, with the aim of extracting the stationary moments of visitors.

The methodology described in this contribution is a foundational step for the broader research objectives of META-MUSEUM.

Although the use of UWB technology is well established both in the scientific literature and in professional applications, including museum-related contexts, the present study introduces several innovative aspects. First, the proposed system is based on low-cost UWB devices, demonstrating that reliable positioning performance can be achieved without relying on expensive, high-end hardware. This aspect is particularly relevant for cultural heritage and museum applications, where budget constraints often limit the adoption of advanced tracking technologies. A second key contribution concerns the management of time synchronization issues. Unlike many existing studies that assume perfect time

synchronization among all devices, in this work we explicitly consider a scenario in which time synchronization between different sensors is not available, including heterogeneous devices such as UWB tags and an eye-tracking system. Finally, the experiments were conducted in a highly challenging and relatively unique environment, characterized by the presence of glass and plexiglass exhibition cases, complex room geometries, and a high density of visitors. These factors introduce signal disturbances, multipath effects, and measurement noise that are often neglected in controlled laboratory settings. By validating the system in such conditions, this study provides evidence of the robustness and practical applicability of the proposed solution in real museum environments.

Future research phases will also consider the physiological results to which the same synchronization methodology will be applied to create a fully integrated system. In this way, spatial behavior and multiple physiological signals can be analyzed together to reveal how cultural heritage experiences affect visitors' emotions and cognition.

2. META-MUSEUM Project: The Need to Localize Visitors in Museums

The indoor localization of people and goods is fundamental for a wide range of applications, spanning safety and emergency management as well as experience enhancement in complex environments such as transportation hubs, educational institutions, and cultural venues. In museums and exhibitions, indoor positioning systems enable location-aware services, including personalized audio guides and context-sensitive digital content triggered by proximity to specific exhibits, thereby supporting visitor engagement and learning.

The META-MUSEUM project is grounded in the recognition that cultural heritage (CH) is a dynamic construct, continuously reinterpreted through social interaction, individual perception, and collective memory. In this context, empathy and emotional engagement play a central role in how cultural experiences are perceived, shared, and internalized by museum visitors.

The project aims to integrate indoor positioning technologies with emotional state monitoring in order to better understand visitor behavior and engagement during museum visits. Using sensors and mobile devices, visitors' physiological responses are collected with informed consent and associated with their spatial trajectories and interaction patterns within the exhibition space.

This data-driven approach provides curators and museum designers with valuable insights, enabling them to craft more engaging, emotionally resonant, and personalized exhibitions. The integration of location-based services with emotional analytics supports informed decisions regarding exhibit placement, interaction design, and narrative development, ultimately fostering more meaningful and immersive cultural experiences.

By analyzing spatial behavior alongside emotional responses, META-MUSEUM also contributes to research on how cultural heritage experiences can promote empathy, reflection, and social cohesion. More broadly, the project supports the transformation of museums into interactive environments where digital technologies complement curatorial practices and visitor-centered design.

In this context, META-MUSEUM aims to implement indoor positioning techniques in conjunction with measuring emotional states in cultural experiences, through the use of sensors and mobile devices, to gather data on visitors' physiological responses (with their previous informed consent): this data can then be combined with information about the visitor's location and behaviour within the museum to obtain a more comprehensive picture of their emotional state.

Achieving these objectives requires first establishing a reliable and accurate indoor localization framework capable of capturing visitor movement with sufficient spatial resolution.

This multidisciplinary approach requires establishing a robust spatial foundation first. Analyzing visitor trajectories, dwell times, and spatial engagement patterns provides a necessary baseline for interpreting how audiences interact with cultural heritage spaces. Subsequently, integrating centimeter-level positioning accuracy with physiological monitoring enables precise correlations between emotional responses and specific locations or exhibit interactions, supporting evidence-based optimization of museum layouts and visitor experiences.

3. Materials and Methods

This section provides a detailed description of the hardware components utilized in the experiment, as well as the methodology used for data collection and analysis.

3.1. Hardware

3.1.1. Ultra-Wideband (UWB) Positioning System

UWB technology is a short-range radio communication system characterized by a large bandwidth exceeding 500 MHz, enabling positioning accuracy at the centimeter level [20]. Position estimation in UWB systems is achieved through various methodologies, all of which rely on geometric principles, such as trilateration or multilateration, to convert signal measurements into spatial coordinates. The three most common measurement techniques include Time of Flight (ToF), Time Difference of Arrival (TDoA),and Angle of Arrival (AoA) [14,20]. Each method has its own advantages depending on the specific application, environment, and required level of accuracy.

For this study, the Single-Sided Two-Way Ranging (SS-TWR) method was selected as the primary methodology. While the fundamental principle relies on ToF, SS-TWR is employed to calculate the distance by measuring the round-trip time of the signal, thereby eliminating the need for strict clock synchronization between the tag and the anchor [21]. This methodology is based on measuring the elapsed time of signals exchanged between the tag and anchor. A basic message communication scheme is illustrated in Figure 1, where the tag is represented by letter T and the anchor by letter A.

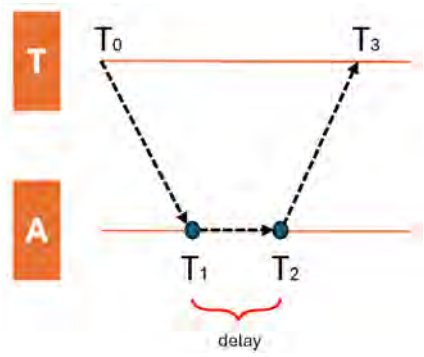

Figure 1. Schematic representation of the ToF measurement, where T represents the tag (mobile device) and A represents the anchor (fixed reference point).

Following this scheme, the tag transmits a signal at timestamp T_0, and the anchor receives the signal at timestamp T_1. After a processing delay $(T_2 - T_1)$, the anchor sends a response at timestamp T_2, and the tag receives the response at timestamp T_3. The ToF is calculated by accounting for the round-trip nature of the signal and removing the processing delay [22]:

$$\text{ToF} = \frac{(T_3 - T_0) - (T_2 - T_1)}{2} \quad (1)$$

The distance between the two devices is then calculated using the following formula:

$$d = c \times \text{ToF} \tag{2}$$

where:

- d is the estimated distance;
- c is the speed of light (c = 299,792,458 m/s).

The accuracy of the range estimations can be affected by NLOS conditions, where obstacles attenuate or reflect the transmitted signal, potentially introducing errors in distance measurements [23]. To mitigate these effects, we applied a dual filtering procedure that targets only the errors we can reliably identify from the available data. Specifically, we performed a spatial boundary check and a statistical feasibility test based on the UWB positioning error ellipse, as will be described in Section 4.1. This approach enables the removal of clearly non-feasible points, such as those falling inside exhibit cases or outside the accessible area, likely caused by strong multipath effects. Future work will extend this analysis by evaluating how the different materials present in the room (e.g., glass, metal) influence the positioning accuracy, enabling a more refined modeling of UWB error behavior in museum environments.

The data acquisition process was carried out using Pozyx® UWB development modules, Figure 2. Pozyx® is a real-time location system (RTLS) that provides centimeter-level accuracy while maintaining low power consumption, making it suitable for indoor environments [20]. The system supports both TWR and TDoA methodologies; for this study, we used TWR, which eliminates the need for clock synchronization between the tag and anchor devices.

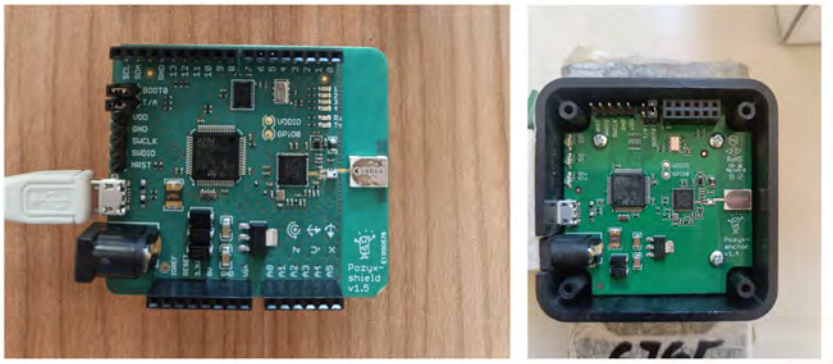

Figure 2. Pozyx tag (**left**), Pozyx anchor (**right**).

We chose the Pozyx® prototype kit specifically because of its affordability, costing a few hundred euros [24], compared to other professional positioning tracking systems that can cost tens of thousands of euros. This makes the approach accessible for museums and research institutions operating with limited budgets. The technical specifications of the Pozyx® modules are shown in Table 1. A Raspberry Pi served as the processing unit, collecting UWB signals, filtering data, and storing visitor trajectory coordinates.

While UWB positioning provides spatial localization data, in this study we chose to operate without the use of absolute timestamps from the low-cost system. The aim was to reproduce a worst-case scenario and test whether it is possible to achieve reliable synchronization between UWB positioning data and eye-tracking recordings.

Table 1. Ultra-wideband Specifications (source: https://www.pozyx.io/, accessed on 5 September 2025).

UWB Pozyx	Details
Transceiver	Decawave DW1000
Chip Antenna	Onboard
Accuracy	Up to 10 cm
Frequency Range	3.5–6.5 GHz
Communication	Up to 6.8 Mbps
Range	Up to 100 m

3.1.2. Eye-Tracking System

To complement the UWB positioning data, Tobii Pro eye-tracking glasses were integrated into the experimental setup (Figure 3). The eye-tracking system provided the temporal reference necessary for validating visit durations and dwell intervals, as well as orientation information that will be fundamental for future behavioral studies. Tobii Pro is a leading technology in eye-tracking research [25], with numerous studies confirming the reliability and accuracy of gaze-tracking applications in various research contexts [26,27]. The technical specifications of the eye-tracking device are presented in Table 2. For this preliminary study, the analysis was limited to extracting visit durations and validating UWB-detected dwell intervals, without examining specific gaze focus points, which will be addressed in future research within the META-MUSEUM project framework.

Table 2. Eye-tracking System Specifications (source: https://www.tobii.com/products/eye-trackers/wearables/tobii-pro-glasses-3, accessed on 5 September 2025).

Eye Tracking Feature	Specification
Eye tracking technique	Corneal reflection, dark pupil, stereo geometry
Sampling rate	50 Hz or 100 Hz
Parallax compensation tool	Automatic
Pupil measurement	Yes, absolute measure
Binocular eye tracking	Yes
Calibration procedure	One point OR automatic calibration
Slippage compensation	Yes, 3D eye tracking mode
Accuracy	0.6°

Figure 3. Tobii Pro Glasses 3.

3.2. Experimental Setup

3.2.1. Environment Characterization and Anchor Geometry Analysis

The experiment was conducted in a room of the Egyptian Museum in Turin, Italy, starting on the 9th of September 2024, in a space measuring approximately 30 m × 9 m with a ceiling height of about 7 m. The room presented a particularly challenging environment for UWB positioning due to the presence of numerous reflective surfaces and obstacles. The exhibition contains 10 glass display cases with Egyptian artifacts, including mummies, sarcophagi, ancient textiles, and various archaeological objects. These glass surfaces can induce significant signal reflections and multipath propagation effects in UWB systems [8], making this an ideal testing environment for evaluating positioning accuracy in a real, non-controlled environment.

For the experiment, we used a single entrance/exit point, allowing for controlled visitor flow management. Each visitor was equipped with a Pozyx UWB tag for positioning data collection and eye-tracking glasses for visit recording. To ensure spatial coverage, ten UWB anchors were installed on the walls and exhibit cases. However, due to museum constraints, the location of the anchors had to be approved by the curators, and they were mounted only in permitted locations.

To evaluate how the geometric configuration of the anchors influences localization accuracy, we performed a horizontal dilution of precision (HDOP) analysis. The HDOP index highlights areas of the room where the anchor geometry provides weaker positioning strength. The computation is based on the least squares method as follows:

For each grid cell, its barycenter is taken as the representative test point:

$$\mathbf{p} = \begin{bmatrix} x \\ y \end{bmatrix}, \quad \mathbf{a}_i = \begin{bmatrix} x_i \\ y_i \end{bmatrix}. \tag{3}$$

where $\mathbf{a}_i$ denotes the position of anchor i. The distance between $\mathbf{p}$ and anchor i is:

$$d_i = \sqrt{(x - x_i)^2 + (y - y_i)^2}. \tag{4}$$

To evaluate the effect of anchor geometry on positioning accuracy, the range observation equations are linearized around the test point. The resulting Jacobian (design) matrix $\mathbf{H}$, composed of the partial derivatives of the distances with respect to the unknown horizontal coordinates, is formed from the normalized direction vectors as follows:

$$\mathbf{H} = \begin{bmatrix} \frac{x - x_1}{d_1} & \frac{y - y_1}{d_1} \\ \frac{x - x_2}{d_2} & \frac{y - y_2}{d_2} \\ \vdots & \vdots \\ \frac{x - x_N}{d_N} & \frac{y - y_N}{d_N} \end{bmatrix}. \tag{5}$$

The geometry (normal) matrix and its inverse are calculated as follows:

$$\mathbf{N} = \mathbf{H}^\top \mathbf{H}, \qquad \mathbf{N}^{-1} = (\mathbf{H}^\top \mathbf{H})^{-1}. \tag{6}$$

From $\mathbf{N}^{-1}$, the coordinate variances are:

$$\sigma_x^2 = [\mathbf{N}^{-1}]_{11}, \qquad \sigma_y^2 = [\mathbf{N}^{-1}]_{22}. \tag{7}$$

Finally, the HDOP is defined as follows:

$$\text{HDOP} = \sqrt{\sigma_x^2 + \sigma_y^2} = \sqrt{[\mathbf{N}^{-1}]_{11} + [\mathbf{N}^{-1}]_{22}}. \quad (8)$$

Assuming a ranging precision of $\sigma_{\text{range}} = 0.10$ m (10 cm), the expected horizontal error is:

$$\sigma_{\text{pos}} = \text{HDOP} \cdot \sigma_{\text{range}}. \quad (9)$$

Figure 4 presents both the HDOP index and the corresponding expected position error distribution across the museum room. The HDOP map (left side of Figure 4) shows higher values in areas where the anchors are positioned too close to one another, resulting in a weaker geometric configuration. Consequently, larger positioning errors are expected in regions with poor anchor geometry.

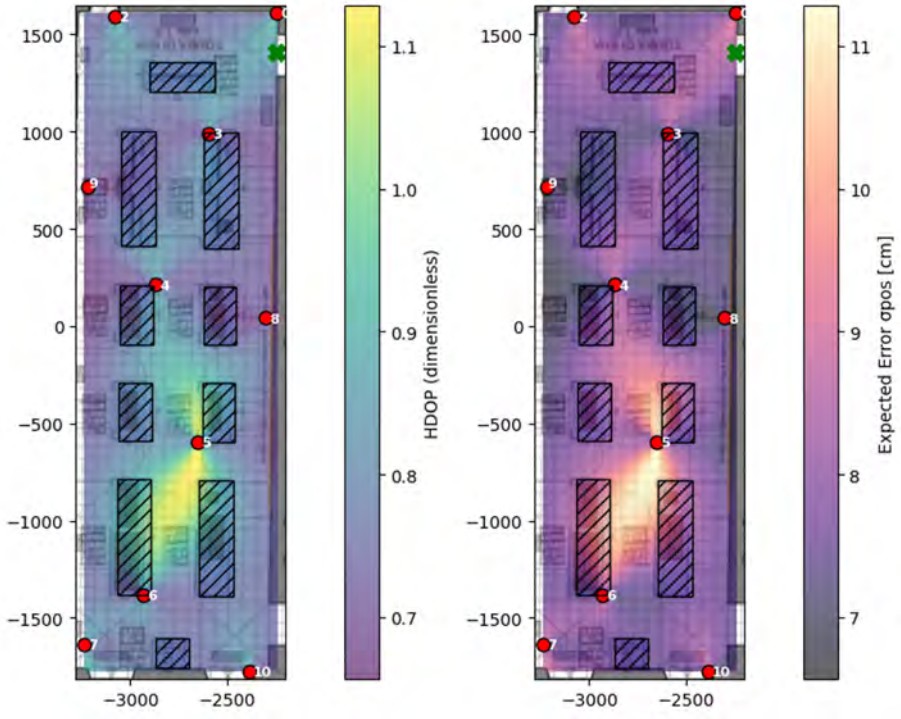

Figure 4. Geometry-based analysis of the anchor configuration in the museum room. (**Left**) Horizontal Dilution of Precision (HDOP) map. (**Right**) Expected position error map.

Our research group had previously investigated for another paper the performance of the range of the UWB using different materials commonly found in museums [28]. That study found that materials such as wood, plexiglass, and glass can introduce ranging errors that exceed 10 cm at distances of up to 30 m, and the errors do not increase linearly with distance. This matters because HDOP analysis only evaluates the geometric arrangement of anchors and cannot account for how signals interact with physical obstacles. In our museum experiment, glass display cases and reflective surfaces created substantial multipath effects that likely had a stronger influence on positioning accuracy than the anchor geometry itself.

3.2.2. Spatial Referencing and Anchor Installation

Following the definition of the experimental constraints and the HDOP analysis, the next step involved the precise installation and referencing of the UWB network. To ensure the spatial coordinates recorded by the UWB system were accurately aligned with the room's physical layout, we first established a high-precision reference frame.This was achieved by using a LiDAR scanner to create a detailed 3D point cloud of the entire room,

which was then accurately georeferenced using a total station. This established the local coordinate system of the museum space. We then used this 3D model (Figure 5) to select the exact locations for the anchors. By manually marking the anchor positions within the 3D, we obtained their high-accuracy coordinates. These coordinates were then used as an input into the Pozyx positioning system's algorithm, allowing the UWB system to use these fixed points for subsequent triangulation and visitor position estimation. Figure 6 shows the workstation of our system and the installation of the anchors in the predefined locations.

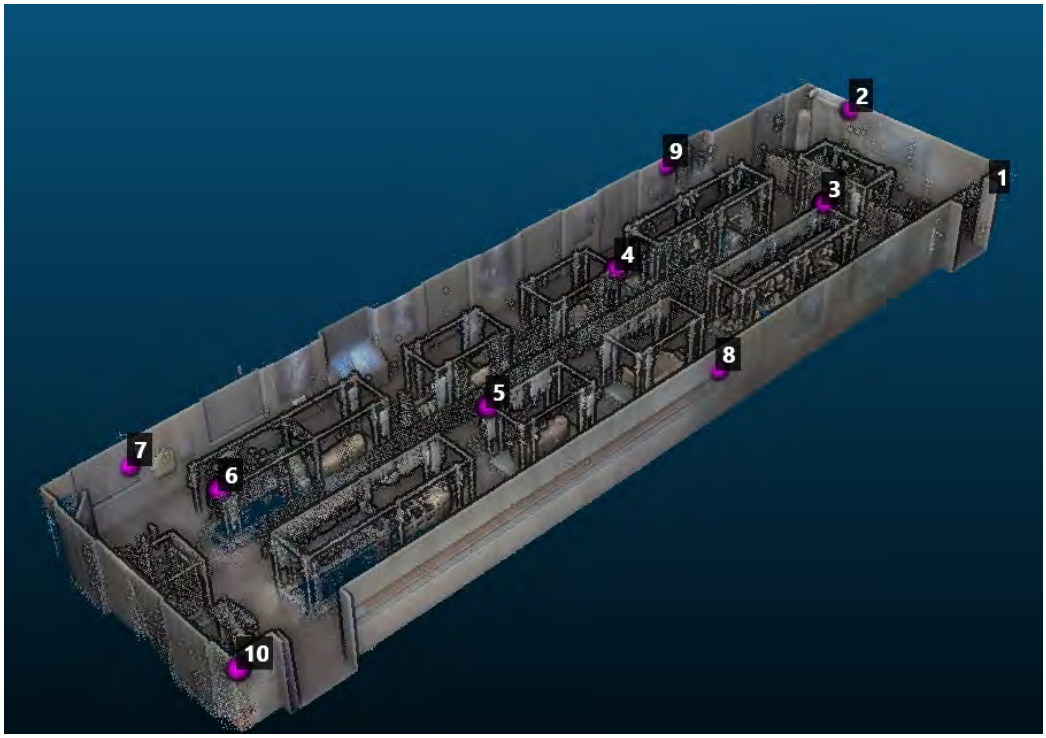

Figure 5. LiDAR-generated 3D point cloud representation of the museum room showing the precise spatial layout and anchor positioning.

Figure 6. Workstation used for monitoring and data collection (**left**). Installation of UWB anchors on the walls to align with LiDAR-determined coordinates (**right**).

4. Results

This section presents the experimental results demonstrating the performance of UWB positioning technology, and the effectiveness of integrating eye-tracking data for a preliminary behavioral analysis.

This study involved 100 museum visitors. To preserve privacy while maintaining representativeness, participants were grouped into seven classes based on demographic and behavioral features (e.g., gender balance, education level, museum-visit habits, visit duration, path length, and dwell behavior). From each class, one visitor was selected as the representative profile for detailed reporting. The overall sample maintained approximate gender balance and included individuals with varying educational backgrounds (60% with high school or higher education; 15% university students) and different levels of museum experience (20% frequent museum visitors). The seven selected visitors spent between 5 and 25 min inside the museum room.

Given that this pilot phase focuses on evaluating UWB performance in a real museum environment, visitors entered at non-overlapping intervals through a single entrance/exit. This controlled design simplified data processing and reduced potential interference, including signal collisions between multiple UWB tags and human-body obstruction effects [28].

4.1. Trajectory Identification

The first goal is to analyze visitor movement patterns within the museum room. Figure 7 illustrates the reconstructed trajectories of the seven representative visitors. To reduce the high-frequency noise, typical of raw UWB measurements, each trajectory was filtered using a rolling mean smoothing method applied to the position coordinates. This approach preserves the overall movement dynamics while removing random oscillations and small fluctuations due to sensor noise or hand motion during tag carrying.

From the trajectories, it is already possible to notice some differences in how visitors moved through the room. Some participants followed relatively smooth and linear paths, suggesting they walked continuously without stopping for long. Others such as Visitors 2, 3, and 6, show paths with several overlaps or loops. These could indicate short pauses, back-and-forth movements, or small oscillations caused by how the UWB tag moved with the arm. This observation is important, because while UWB positioning provides useful spatial information, it does not always allow us to tell whether a visitor actually stopped to observe an exhibit or simply moved slightly within the same area. For this reason, integrating UWB data with eye-tracking recordings becomes essential to determine whether visitors were actively observing a specific exhibit, revisiting a previous location, or remaining stationary in one spot.

4.2. UWB Spatial Heatmaps with Data Filtering

To visually understand and quantify how visitors utilized the museum space, we generated spatial heatmaps representing the density of recorded UWB position points. These heatmaps serve as the initial, clear representation of visitor presence, highlighting areas of frequent movement and stationary behavior.

The reconstructed trajectories reveal an immediate problem, which is the presence of positioning solutions inside exhibit cases or outside the room entirely. This is mainly caused by the reflective materials of the museum environment, especially the glass display cases, which can distort the UWB signal and produce both random noise and systematic errors due to multipath effects. To make sure the analysis represents real visitor movement, these unrealistic coordinates were filtered out to avoid confusing signal artifacts with actual positions.

To quantify the extent of these outliers, a combined spatial and statistical filtering approach was implemented, Figure 8. Coordinates located outside of the room boundaries are represented by red crosses and they are filtered out due to physical constraints. For coordinates located within exhibit cases, a statistical feasibility test was applied. This test utilized the UWB positioning error ellipse based on the device's positioning uncertainty ($\sigma_x, \sigma_y \approx 5$ cm). If 75% (3/4) or more of this error ellipse fell within the exhibit case boundaries, the coordinate was classified as a statistical outlier and filtered out. This approach recognizes that while UWB measurements have inherent uncertainty, points whose error ellipses are predominantly contained within inaccessible areas are likely erroneous measurements caused by multipath effects from glass surfaces. By applying this dual filtering methodology, we combined a physical boundary check together with statistical analysis to guarantee that only valid coordinates are considered for the spatial heatmap. Table 3 provides the percentage of these outliers relative to the total recorded coordinates for each visitor.

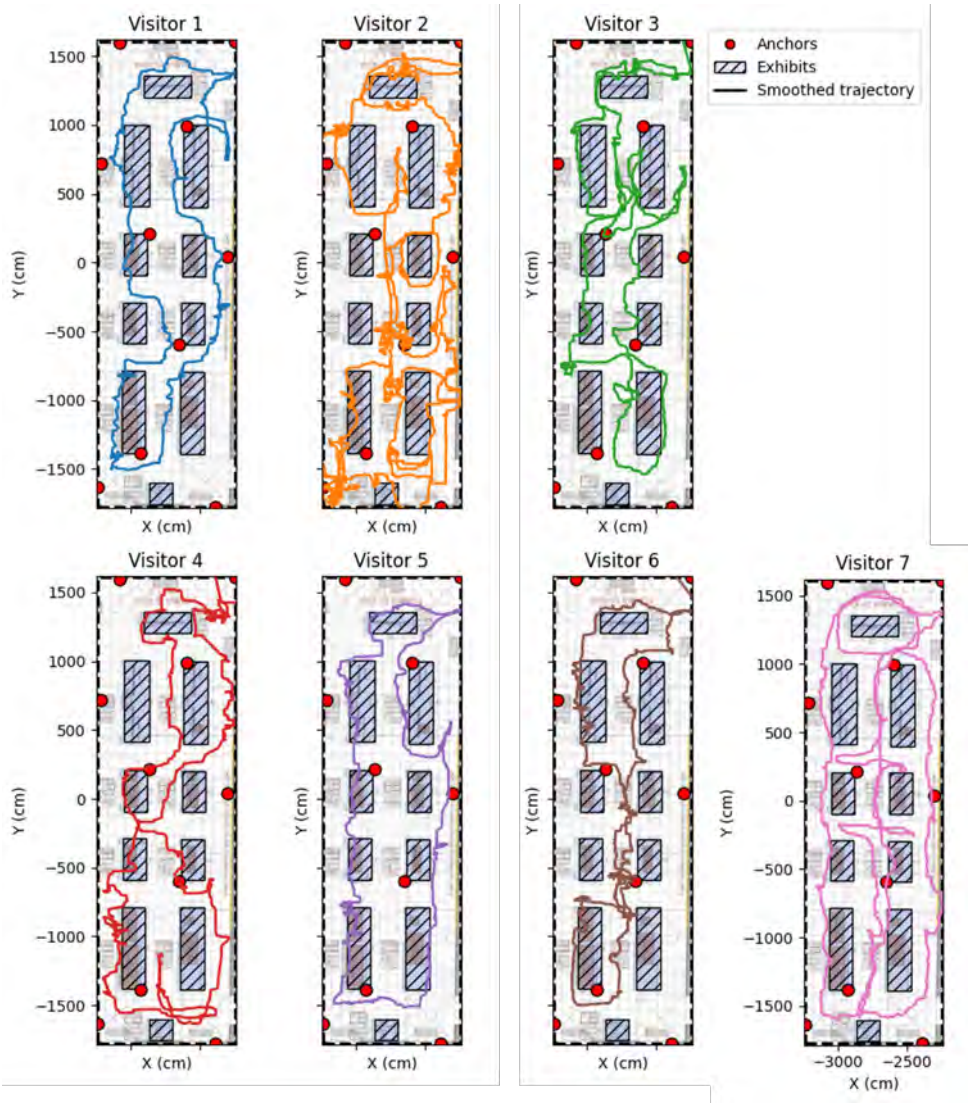

Figure 7. Individual reconstructed trajectories of the seven representative visitors. Each panel corresponds to a different participant (Visitors 1–7), and shows the smoothed UWB-based trajectory of that specific visitor within the museum room. Red circles indicate UWB anchor positions, while gray hatched areas represent exhibit locations.

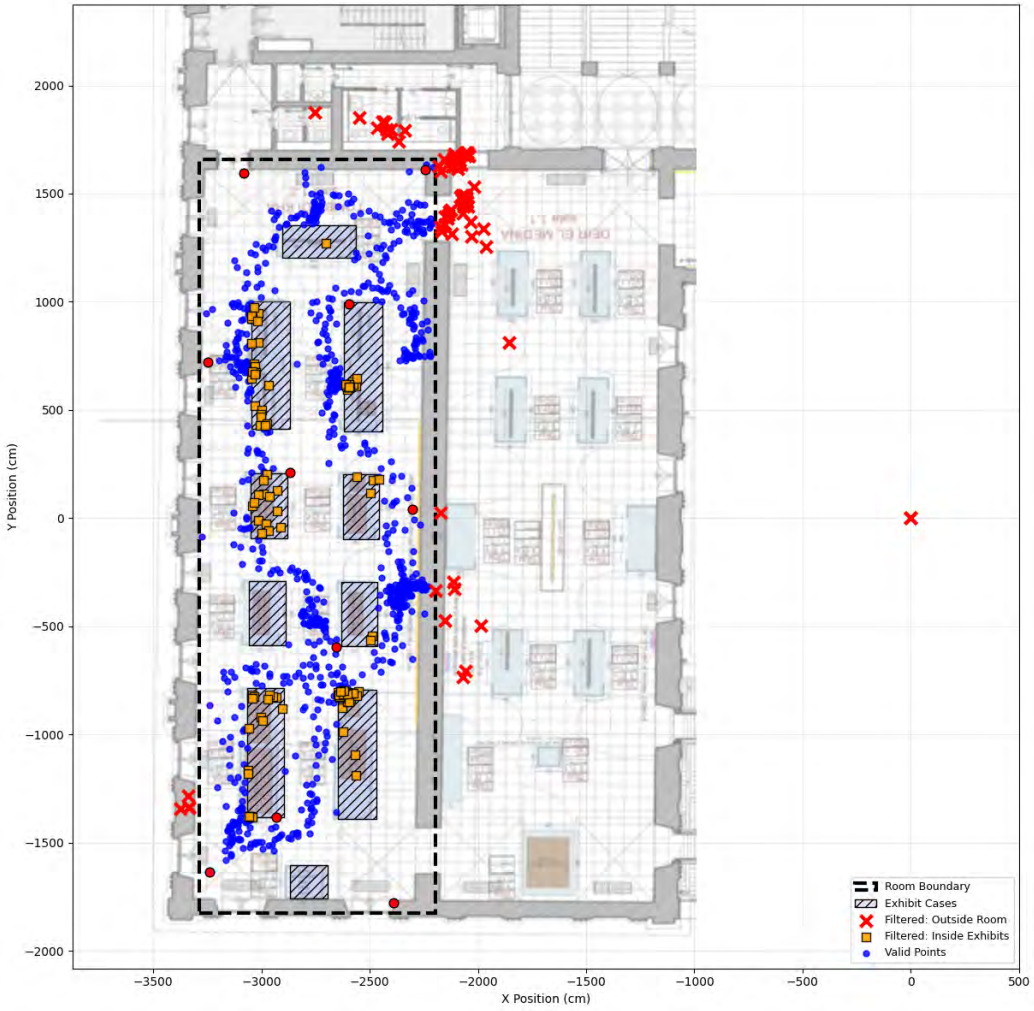

Figure 8. Combined spatial and statistical filtering methodology for outlier rejection applied to visitor V1 coordinate data.

Table 3. Visitor's Non Feasible Points Percentage.

Visitor id	Percentage of Outliers (%)	Total Points
V1	11	1259
V2	6	6109
V3	10	1708
V4	8	1350
V5	22	1639
V6	13	1947
V7	4	1415

The filtered spatial heatmaps in Figure 9 highlight the areas where visitors spent the most time, with darker red regions showing higher point densities that correspond to longer stays or frequent passages. It is important to note that this filtering process applies only to the spatial heatmaps, which are intended to provide a clean visual representation of visitor presence. In the next analyses, such as dwell-time estimation or synchronization with eye-tracking data, all recorded samples are retained. Even small oscillations around a true position are meaningful, as they contribute to the total duration a visitor spends in a specific area and removing them would underestimate the actual observation time.

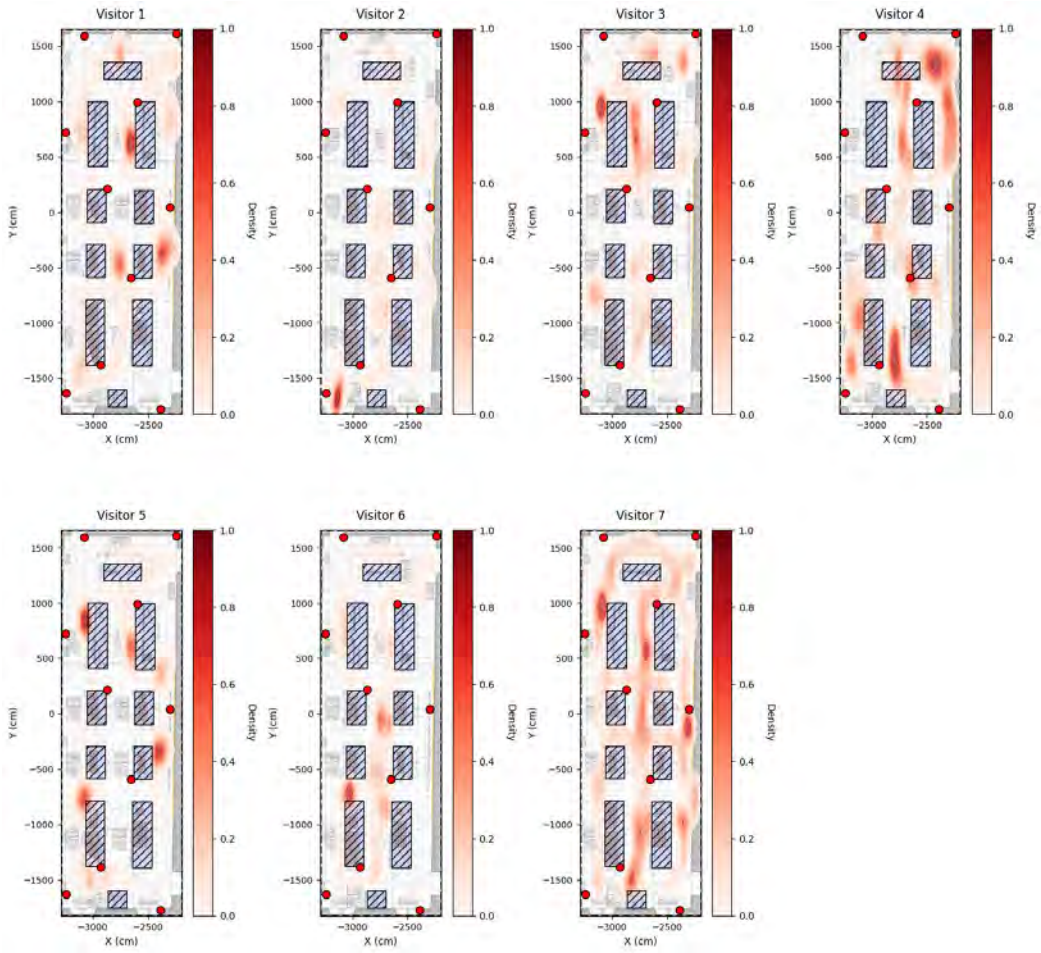

Figure 9. Individual visitor heatmaps for V1, V2, V5, and V6 after filtering out outliers located inside exhibit cases and outside room boundaries. The color intensity represents the density of recorded coordinates, with darker red areas indicating zones of higher visitor activity.

4.3. Preliminary Detection of Dwell Intervals from UWB Data

While spatial heatmaps offered a general view of frequently visited areas, they lacked information on visitor engagement duration. To explore this temporal aspect, we identified and analyzed the periods during which visitors were stationary. This dwell time analysis required keeping all recorded positions within the room boundaries, including those located inside the display cases. This choice was made because the temporal analysis focuses on the duration of presence rather than precise spatial accuracy, and every recorded sample contributes to understanding how long visitors stayed in proximity to specific exhibits.

The approach focuses on analyzing the temporal variation in UWB range measurements. Each estimated visitor position is associated with a set of range values measured between the visitor-worn tag and the fixed anchors, representing the distance to each anchor at a given time instant. Stationary behavior, characterized by minimal movement, was identified by detecting plateau patterns in the range values over a minimum duration:

$$T_{\text{dwell}} \geq 10 \text{ s} \tag{10}$$

To ensure robust detection, the algorithm was tuned using visitor-specific parameters, including tolerance (to account for minor range fluctuations), the sampling interval, and a window size for signal smoothing. Specifically, plateau detection was implemented using a sliding temporal window in which the absolute variation in the range signal was required to remain below a predefined tolerance threshold for at least T_{dwell}. This condition indicates

sustained minimal movement and is consistent with stationary visitor behavior. Plateau detection was applied consistently across the available anchors, and a dwell event was confirmed only when plateau conditions were satisfied by a majority of anchors, reducing sensitivity to anchor-specific noise and measurement artifacts.

The plateau detection result is illustrated in Figure 10, where green highlighted regions indicate the identified stationary periods across the anchor network. This figure uses nine anchors rather than the complete set of ten, as the fifth anchor consistently returned zero values for all participants, indicating a potential malfunction or signal obstruction that made it unusable for range-based analysis.

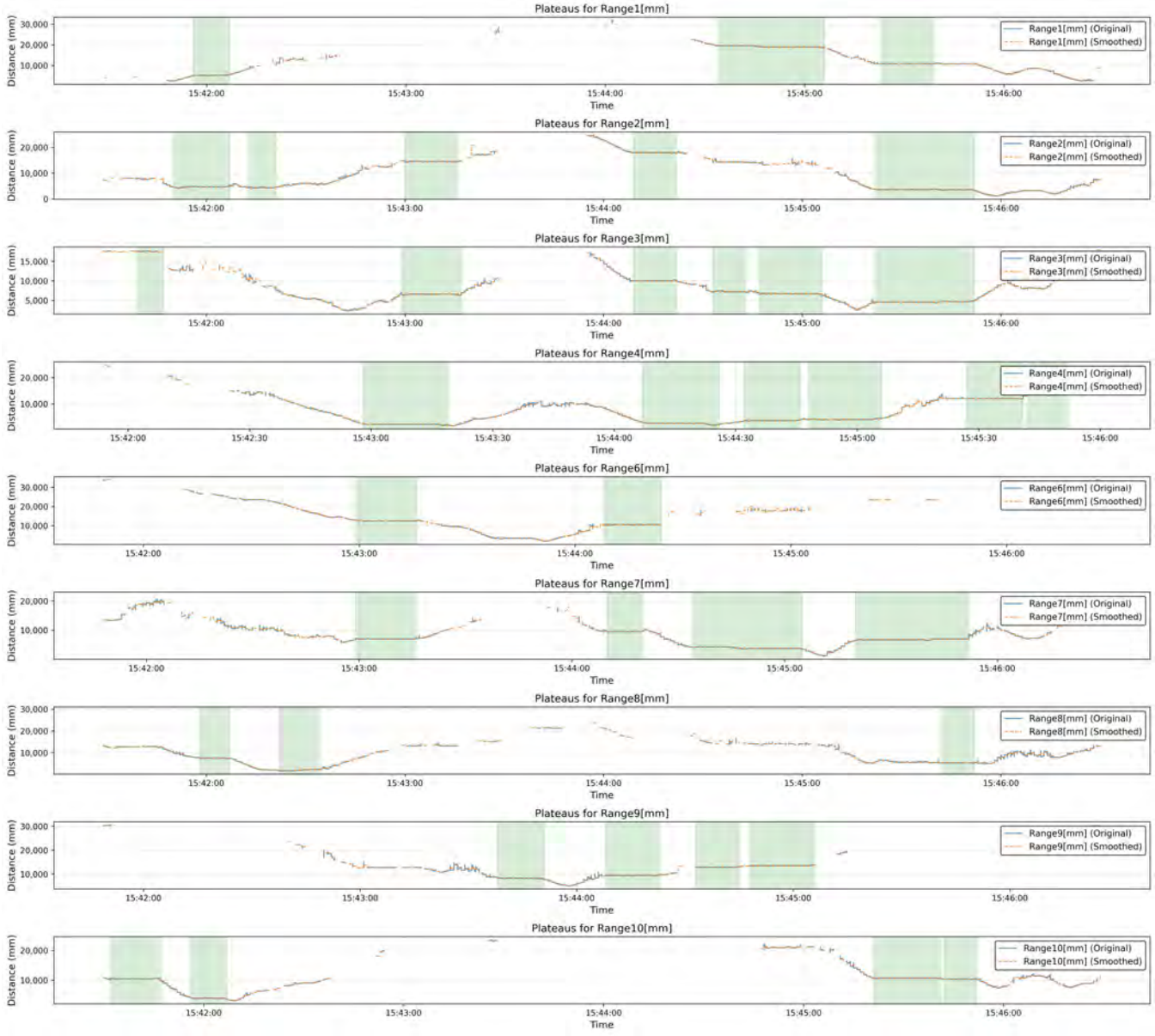

Figure 10. Plateau detection analysis for visitor V1, showing range measurements from nine functional anchors (anchors 1–4 and 6–10), with green highlighted regions indicating identified stationary periods.

The coordinates linked to these time interval plateaus were then classified as dwell time intervals. To provide a spatial representation of these intervals, the corresponding coordinates were mapped to the planimetry, as shown in Figure 11. This spatial mapping reveals the precise locations where visitors exhibited stationary behavior, enabling the

identification of high-engagement zones within the museum space. It is important to note that in this pilot study, the parameters used for plateau detection were individually adjusted for each representative visitor to establish an optimal detection threshold. This calibration was necessary to identify suitable values for different movement patterns. In future implementations, these parameters will be standardized based on the results of this calibration, and adaptive algorithms will be introduced to automatically adjust their values according to visitor behavior.

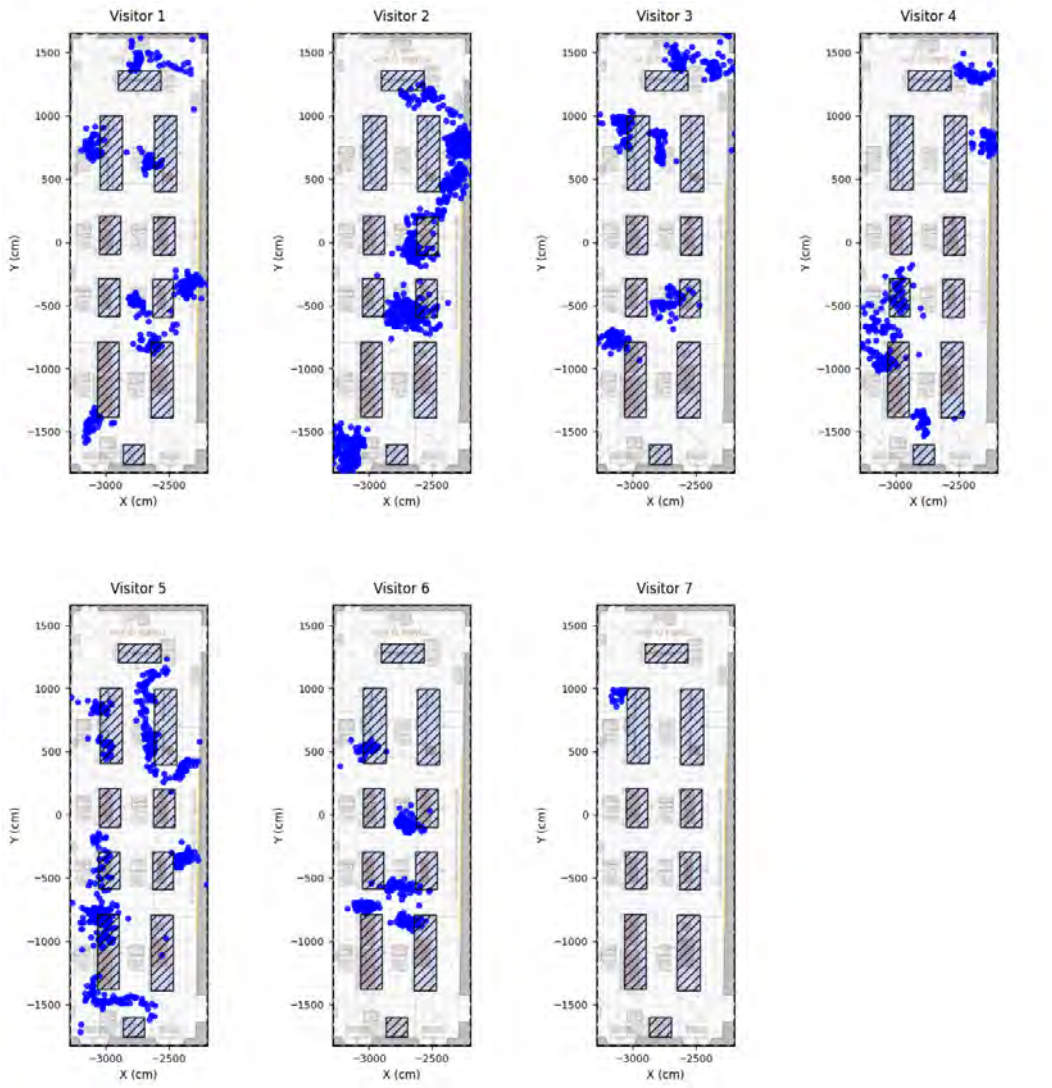

Figure 11. Visitor V1 dwell interval coordinates mapped onto the museum room floor plan, showing the spatial locations where stationary behavior was detected.

The Pozyx UWB system and the eye-tracking glasses are independent devices, operating without automatic synchronization. This independence, combined with the UWB system's use of a relative internal clock and a non-constant sampling frequency across visitors, rendered its raw timestamps unreliable for absolute timing. Consequently, the eye-tracking video was used as the ground-truth temporal reference for two critical purposes. Firstly, to accurately determine the duration of detected dwell intervals, and secondly to validate the reliability of the plateau detection algorithm against visual evidence of actual stationary behavior.

4.4. Data Fusion Between UWB and Eye-Tracking Technology

To accurately estimate how long each visitor remained stationary, the UWB data were combined with the eye-tracking recordings, which served as the reference for time synchronization. Since the UWB system started collecting data about three minutes before the eye-tracking videos, the initial UWB coordinates recorded before the visitor entered the room were removed. This ensured that only data corresponding to the visitor's actual time inside the room were used in the analysis.

To reconstruct a consistent timeline for the UWB data, we then calculated the average sampling frequency (f_s) needed to evenly distribute all valid UWB samples over the known duration of the corresponding video (T_{video}). Each coordinate was then assigned a sequential timestamp based on this frequency, preparing the dataset for synchronization with the eye-tracking data.

$$f_s = \frac{\text{Total Number of Valid Samples}}{T_{\text{video}}} \tag{11}$$

This approach relies on the assumption that the UWB sampling rate remained approximately constant and that coordinates were recorded continuously throughout the visit. We acknowledge that this method has limitations as it does not account for potential data loss, signal interruptions, or variations in positioning accuracy, which can distort the assumption of uniform temporal distribution.

Figure 12 illustrates the temporal discrepancy between the two datasets, using visitor V1 as a representative example of the synchronization challenge. It is evident that the UWB plateau detection algorithm, detects a higher number of stationary intervals (blue bars) compared to the visually confirmed pauses from the video recordings (orange bars). This difference highlights the sensitivity of the detection algorithm to parameter selection, and emphasizes the need for a calibration method to minimize inconsistencies.

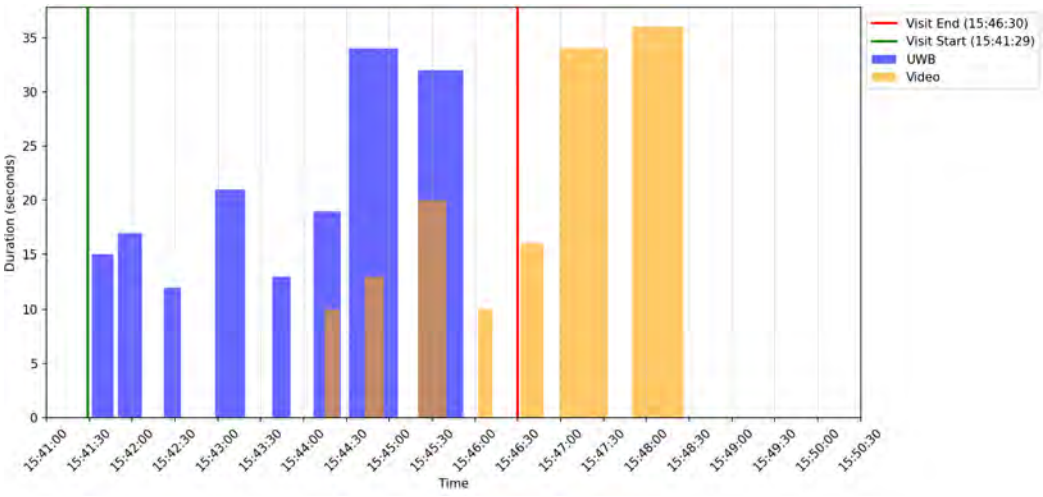

Figure 12. Intervals from both datasets for visitor V1, showing their 3-min time offset and the corresponding durations for each extracted interval.

To align the stationary periods detected by both sensors, the UWB and eye-tracking recordings were transformed into binary signals, assigning a value of 1 to stationary moments and 0 to movement. For the video data, stationary phases were manually annotated only when the pause lasted at least 10, as in Formula (10). Expressing both datasets in this simplified form allowed for a straightforward, event-based comparison between them. Applying a single fixed time offset would not be sufficient as small differences in the UWB sampling rate and the visitor's actual pace could cause the two signals to drift apart over

time. To obtain a more accurate synchronization, we performed a cross-correlation analysis, testing a range of possible time shifts to find the one that maximized the similarity between the two signals. The aligned results (Figure 13 illustrates visitor V1 synchronization result) confirm that this approach effectively compensates for both the initial timing mismatch and the intrinsic differences between the two measurement systems.

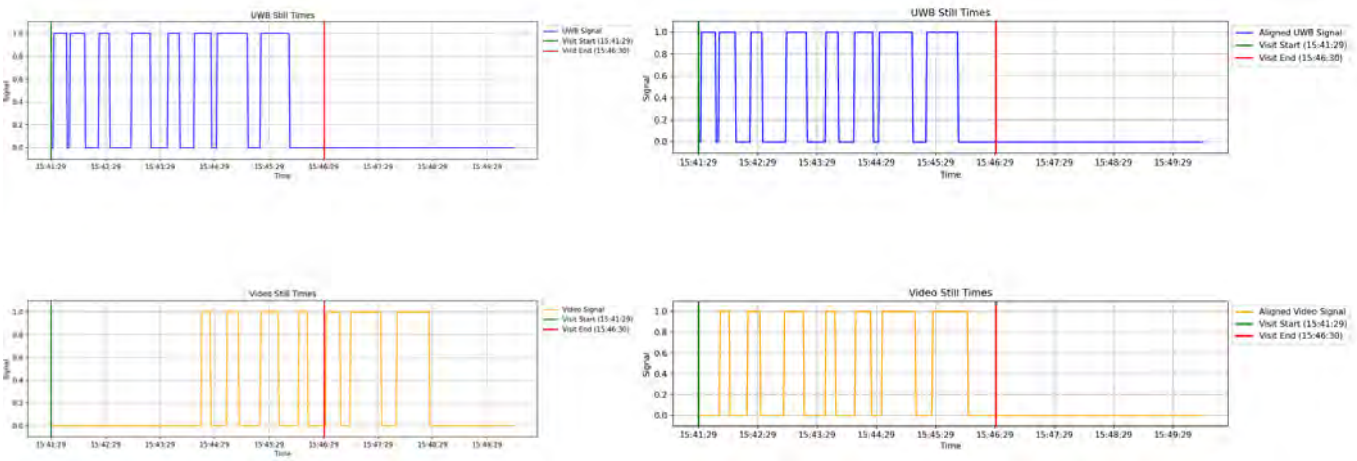

Figure 13. Dwell intervals before (**left**) and after (**right**) the synchronization for visitor V1.

The quality of the alignment was assessed through both temporal and spatial validation metrics summarized in Table 4. The temporal agreement was quantified by the maximal Pearson correlation coefficient (r) achieved during the cross-correlation optimization, ranging from 0.42 to 0.91. This range demonstrates a clear correspondence between the synchronized stationary phases. Correlations above 0.7 (V1, V5, V6, and V7) indicate very good temporal alignment, while moderate values found for V3 and V4 (around 0.4) are likely related to shorter or partially overlapping stationary intervals. Complementing this, the spatial agreement, calculated as the percentage of unique coordinates that overlapped between the synchronized UWB and video intervals, was estimated from 24.52% to 80.20%. Overall, these results confirm the reliability of the synchronization process, establishing a robust foundation for subsequent dwell interval analysis.

Table 4. Pearson correlation coefficients and overlap percentages between UWB and eye-tracking signals after synchronization.

Visitor Id	Pearson Coefficient (r)	Overlap (%)
V1	0.72	66.07
V2	0.65	64.68
V3	0.45	40.01
V4	0.42	24.52
V5	0.79	80.20
V6	0.72	65.79
V7	0.91	76.47

4.5. Clustering-Based Temporal Heatmaps

Based on the previosuly described synchronization method, this paragraph is focused on converting the validated UWB coordinates into quantitative dwell time estimates. The UWB position data still retained spatial noise and scatter, compromising the accuracy of the final dwell time estimation. To address this, a clustering procedure was implemented to spatially refine the identification of the stationary areas by isolating and removing

these spatial outliers. The method employed was the Density-Based Spatial Clustering of Applications with Noise (DBSCAN). DBSCAN method is able to define dense clusters and classify low-density points as noise. This exclusion of outliers was critical to prevent the overestimation of dwell time that would result from counting transient or scattered points. Figure 14 illustrates the resulting stationary zones for all visitors.

Figure 14. Clustering result considering UWB and video dwell intervals.

Once the clusters were defined, the stationary time for each region was calculated. This estimation was based on the inverse of the effective sampling frequency($1/f_s$) from Equation (11), represents the time duration of a single UWB sample. We then derived the total dwell time for each cluster by multiplying the cluster's point count by this inverse

sampling frequency. The resulting heatmaps, shown in Figure 15, illustrate the estimated dwell times based on the combined UWB and eye-tracking data.

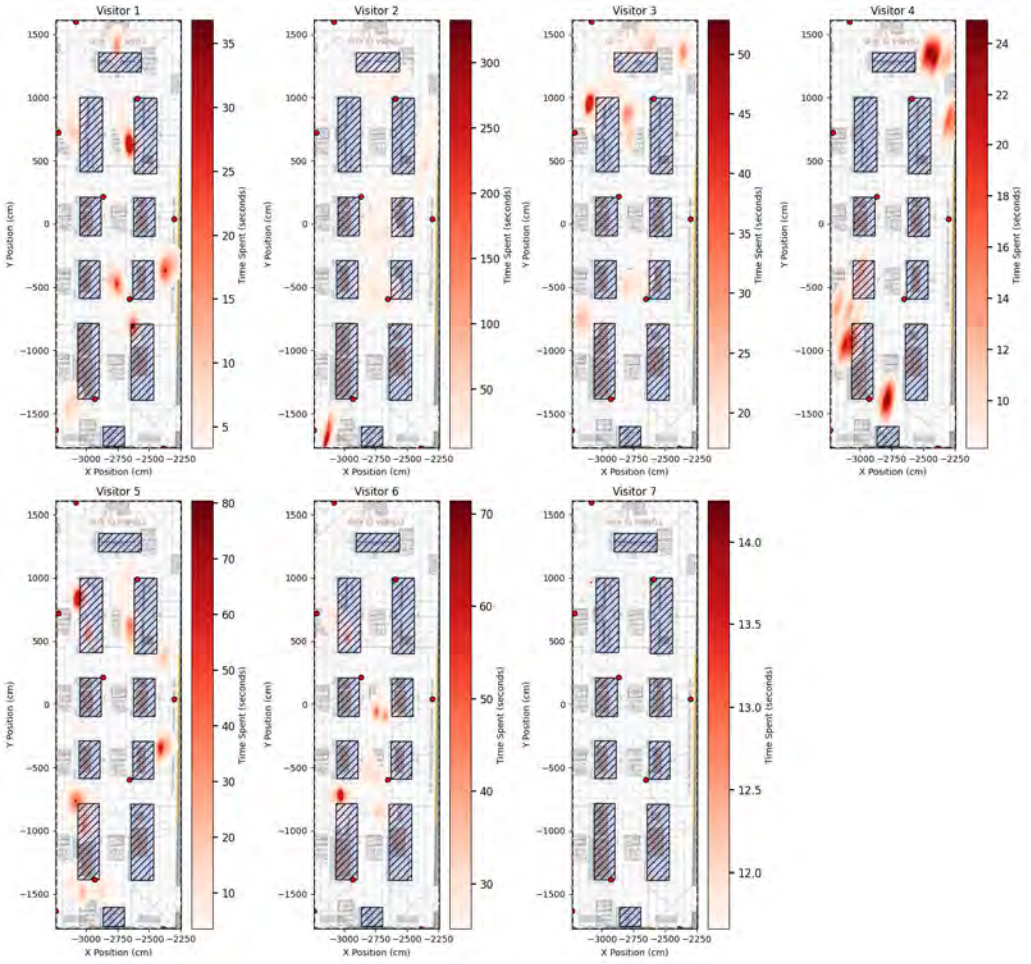

Figure 15. Temporal Heatmaps considering UWB and Eye Tracking devices.

4.6. Normalized Engagement Analysis

Directly comparing absolute dwell times across visitors is not representative to quantify the general overall engagement in the museum room as each visitor spent different amount of time inside the room. To account for the different durations and ensure a fair comparative analysis between the visitors, a normalization process was applied to transform the absolute measurements into relative engagement metrics, as defined in the Formula (12):

$$E_{i,j} = \frac{N_{i,j}}{N_{i,total}} \times 100 \tag{12}$$

where:

- $E_{i,j}$ represents the normalized engagement of visitor i in spatial cluster j;
- $N_{i,j}$ is the number of dwell positions within that cluster j for visitor i;
- $N_{i,total}$ is the total number of valid tracking positions for visitor i.

This normalization ensures that each visitor contributes equally to the comparative analysis, with individual engagement percentages summing to 100% regardless of visit length. The approach enables the identification of areas where visitors concentrated their attention relative to their own behavioral patterns.

The resulting Normalized KDE heatmap for all visitors (left side of Figure 16) illustrates the challenge of interpreting data in a non-controlled environment. Even after

normalization, the map remains susceptible to the influence of highly focused individuals who have disproportionately long visit durations (such as Visitor 2, who spent 25 min compared to the 6-min average). The distinct hotspot in the lower-left area mainly reflects this visitor's extended attention in that specific zone, while most other participants spent only brief periods there. This example shows how, in uncontrolled museum environments, longer visits can shape the collective representation of visitor engagement.

In contrast, the second heatmap (right side of Figure 16) was produced in a controlled environment considering only the visitors with similar visit durations. This map highlights the areas that drew the attention of most visitors, showing where time was spent collectively. The color scale indicates the density of the normalized engagement, revealing the zones where visitors dedicated the largest share of their visit. By excluding the longest visit, the map provides a clearer and fairer picture of common visitor behavior, reducing the bias caused by differences in visit duration.

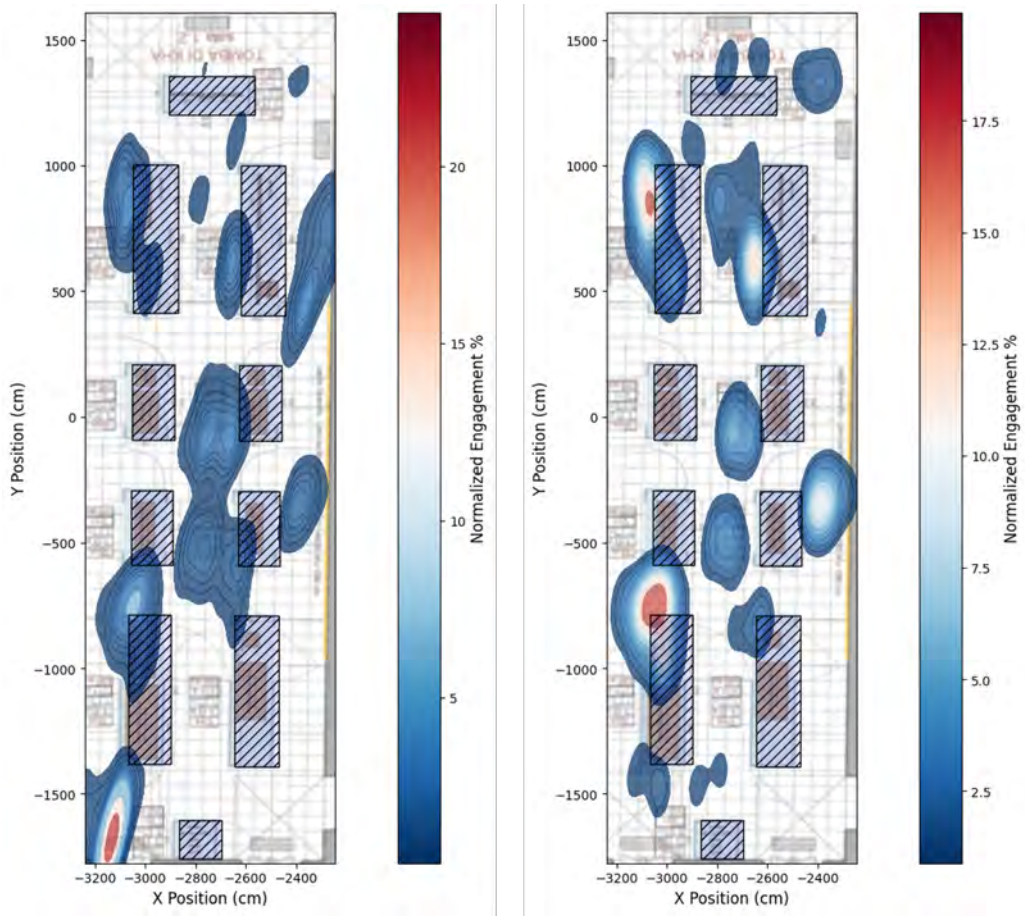

Figure 16. Normalized engagement heatmap for all 7 visitors (**left**). Normalized engagement heatmap for 6 visitors (**right**).

4.7. Collective Engagement Analysis

To identify locations of shared interest across visitors, we applied a further clustering approach. Individual dwell clusters from Section 4.5 were grouped spatially using DBSCAN with a 2 m tolerance radius, accounting for natural positioning variation around exhibits. For each aggregated location, we counted the presence of unique visitors to obtain a collective engagement map.

This analysis differs from the normalized heatmap, which shows how long each visitor spent in different areas. The collective engagement map instead focuses on which locations attracted visitors the most, regardless of how long they stayed. As shown in

Figure 17, the color of each circle represents the number of visitors, while the dashed outline indicates the average spatial spread of dwell points in that area. The results show that the most frequently shared engagement zones were located near Exhibit B3, along the central corridor between Exhibits B7, B8, and close to exhibit B9. Some of these clusters lie at the intersection of multiple display areas, suggesting that positioning data alone cannot determine which exhibit the visitors were actually observing. This demonstrates the importance of integrating eye-tracking analysis to accurately interpret visitor orientation and visual attention.

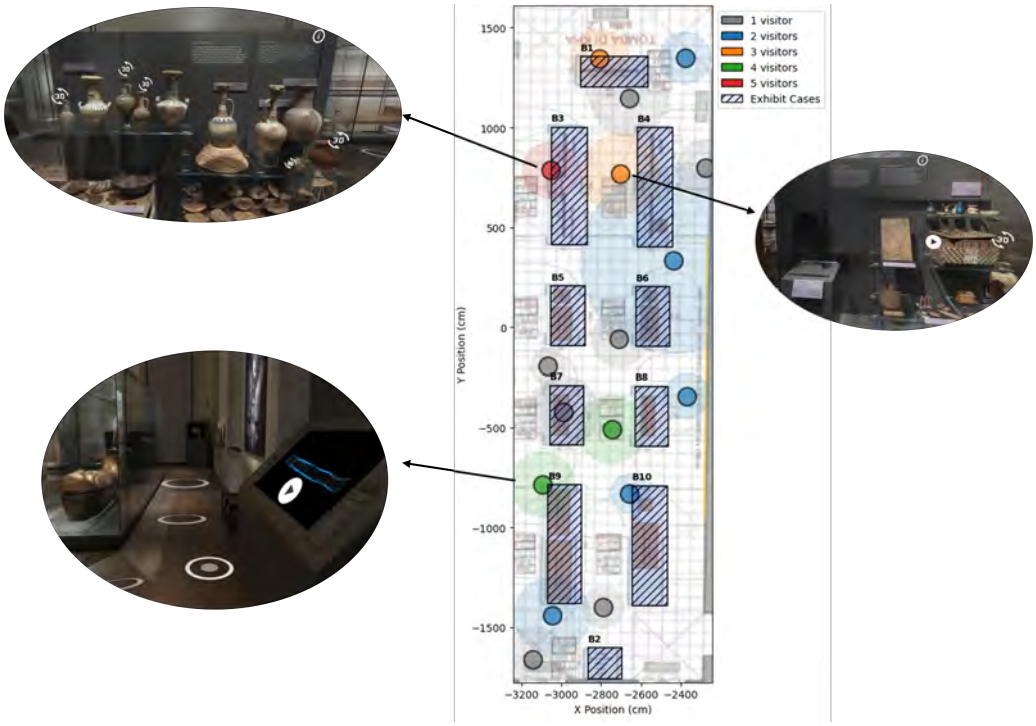

Figure 17. The map displays areas where multiple visitors stopped for extended periods. Circle color indicates the number of unique visitors present (see legend), and the dashed radius represents the average spatial spread of their dwell points. The images of the exhibits are extracted from the Museo Egizio's Virtual Tour (https://virtualtour.museoegizio.it/, accessed on 3 September 2025).

5. Discussion

The heatmap results from the previous section demonstrate the methodological path required to obtain meaningful behavioral data from the UWB system and its fusion with the eye tracker. Our approach adopted two complementary interpretations, the spatial and the temporal one, to analyze visitor engagement effectively.

The spatial interpretation focused first on mapping visitor movement, revealing that recorded positions often appeared inside the exhibit cases. This confirmed that the UWB signal was affected by multipath effects caused by the glass and other obstacles in the room (Table 3). Quantifying these "non-feasible" points was therefore essential to understand system's performance in a real museum environment and to justify the filtering procedures applied to obtain a clean trajectory base.

The temporal interpretation aimed to detect when visitors remained stationary by applying a plateau detection algorithm. A 10 s threshold was chosen as the minimum time a visitor would stay in front of an exhibit to be considered engaged. However, using only UWB data for this step is incomplete, as the positioning data can only provide the visitor's location, not their visual orientation or focus. To improve the reliability of the dwell intervals, eye-tracking data was used as a complementary method to verify the duration of pauses, using the intervals extracted from the videos as the ground truth.

Based on these 2 datasets, we considered two distinct metrics to provide a comprehensive profile of visitor behavior. For the first metric, we applied a normalization process (Figure 16) that accounts for the different time each person spent in the room. This transformation converted the raw dwell times into a measure of relative attention, highlighting which areas received a higher share of each visitor's focus. This step was essential, as the first normalized map revealed that longer visits still had a strong impact on the overall results. In real museum conditions, normalization alone cannot completely remove the bias introduced by varying visit durations. For this reason, we applied the same normalization method to a subset of data representing a controlled visit duration, which provided a clearer picture of where visitors collectively dedicated the greatest proportion of their individual visit time.

The second metric, the collective engagement map, focused on measuring how many visitors were attracted to each location. This serves as a complementary result of the normalization heatmap as it provides insights on locations where visitors acknowledge the exhibit but they might have not dedicate a significant portion of their individual visit time. An area that presents a high number of visitors (Figure 17) but a relatively low normalized engagement percentage (Figure 16) implies a location that serves as a short stopping point or transient observation spot. Visitors acknowledge the exhibit but do not dedicate a significant portion of their individual visit time. In contrast, an area with a high visitor count and a high normalized percentage represents a robust consensus, demonstrating that the location is popular and highly engaging.

6. Conclusions and Future Work

This study presents an evaluation of the UWB positioning technology as the fundumental step for visitor behavioral analysis in cultural heritage environments, conducted within the META-MUSEUM project framework. The experimental campaign was carried out in a real museum setting characterized by complex spatial layouts and the presence of highly reflective materials, such as glass and plexiglass exhibition cases, which represent a challenging scenario for indoor positioning systems.

These preliminary results confirmed the high impact of a complex environment on UWB signal integrity and highlighted the necessity for developing error correction methods based on the influence of materials. The presence of non-feasible coordinates within exhibits demonstrated the signal's susceptibility to interference and multipath effects. Based on these findings, our research group has further investigated UWB signal behavior with various common museum materials, such as glass and plexiglass [28]. Additionally, integrating UWB with complementary sensors demonstrated the need for precise synchronization to ensure robust data collection and reliable ground truth validation. Addressing these challenges and refining sensor fusion techniques will be essential for creating scalable and reliable indoor positioning systems for practical cultural heritage applications.

Beyond the technological assessment, the proposed approach provides concrete benefits for museum operators and curators. The generated heatmaps and dwell-time analyses enable the identification of the most densely occupied areas and the most attractive cultural assets, supporting scientific studies on visitor behavior as well as operational decision-making. From a safety and security perspective, these insights can assist in monitoring visitor flows and detecting potential overcrowding, contributing to improved crowd management in high-density areas. Furthermore, these results can support museum managers and exhibition designers in reorganizing and optimizing the spatial distribution of cultural assets, with the goal of enhancing both the quantity and quality of the exhibition and improving the overall visitor experience.

https://doi.org/10.3390/ijgi15010033

Future research will prioritize investigating how different materials, such as glass display cases, and the presence of human bodies affect UWB signal propagation, with the aim of improving measurement accuracy. Additionally, efforts will focus on developing an enhanced positioning algorithm to avoid filtering out solutions, thereby enabling more precise coordinate restitution. The integration of eye tracking technology to capture visitors' points of focus, combined with additional sensors to monitor physiological signals and positional information, could offer a significant contribution to a deeper behavioral analysis.

Author Contributions: Conceptualization, Paolo Dabove and Vincenzo Di Pietra; methodology, Vincenzo Di Pietra and Paolo Dabove; software, Angeliki Makellaraki; validation, Angeliki Makellaraki, Milad Bagheri and Vincenzo Di Pietra; formal analysis, Angeliki Makellaraki, Milad Bagheri and Vincenzo Di Pietra; investigation, Paolo Dabove and Vincenzo Di Pietra; resources, Paolo Dabove and Vincenzo Di Pietra; data curation, Angeliki Makellaraki and Paolo Dabove; writing—original draft preparation, Angeliki Makellaraki; writing—review and editing, Paolo Dabove and Vincenzo Di Pietra; visualization, Angeliki Makellaraki and Milad Bagheri; supervision, Paolo Dabove; project administration, Paolo Dabove; funding acquisition, Paolo Dabove All authors have read and agreed to the published version of the manuscript.

Funding: This work is part of the research conducted in the framework of META-MUSEUM [101132488–META-MUSEUM 'Moving Emotions towards confidence in the Transformative Appropriation for a Meaningful Understanding of cultural heritage: a neuroScientific approach to EUropean Museums'–HORIZON-CL2-2023-HERITAGE-01] funded by the European Union. Views and opinions expressed are, however, those of the authors and do not necessarily reflect those of the European Union or European Research Executive Agency (REA). Neither the European Union nor the granting authority can be held responsible for them.

Informed Consent Statement: Informed consent was obtained from all subjects involved in this study. All data and participants have been considered anonymously.

Data Availability Statement: The raw data supporting the conclusions of this article will be made available by the authors on request.

Acknowledgments: The authors gratefully acknowledge Valentina Turina and all the staff members of the Egyptian museum in Turin for their help, kindness and valuable support during all the phases of the data collection as well as for giving us the possibility to conduct the experiments in that prestigious location.

Conflicts of Interest: The authors declare no conflicts of interest.

References

1. Grossi, E.; Blessi, G.; Sacco, P.L. Magic Moments: Determinants of Stress Relief and Subjective Wellbeing from Visiting a Cultural Heritage Site. *Cult. Med. Psychiatry* **2019**, *43*, 4–24. [CrossRef] [PubMed]
2. Li, X.; Wang, P.; Li, L.; Liu, J. The influence of architectural heritage and tourists' positive emotions on behavioral intentions using eye-tracking study. *Sci. Rep.* **2025**, *15*, 1447. [CrossRef] [PubMed]
3. Centorrino, P.; Corbetta, A.; Cristiani, E.; Onofri, E. Managing Crowded Museums: Visitors Flow Measurement, Analysis, Modeling, and Optimization. *arXiv* **2020**, arXiv:2006.16830. [CrossRef]
4. Ivanov, R.; Velkova, V. Analyzing Visitor Behavior to Enhance Personalized Experiences in Smart Museums: A Systematic Literature Review. *Computers* **2025**, *14*, 191. [CrossRef]
5. Hailu, T.G.; Guo, X.; Si, H.; Li, L.; Zhang, Y. Theories and Methods for Indoor Positioning Systems: A Comparative Analysis, Challenges, and Prospective Measures. *Sensors* **2024**, *24*, 6976. [CrossRef] [PubMed]
6. Witrisal, K.; Hinteregger, S.; Kulmer, J.; Leitinger, E.; Meissner, P. High-accuracy positioning for indoor applications: RFID, UWB, 5G, and beyond. In Proceedings of the 2016 IEEE International Conference on RFID (RFID), Shunde, China, 21–23 September 2016; pp. 1–7. [CrossRef]
7. Gamarra, M.V.; Papaharalabos, S.; Rezaei, F.; Bartlett, D.; Karlsson, P. Seamless Indoor and Outdoor Positioning with Hybrid Bluetooth AoA and GNSS Signals. In Proceedings of the 2023 13th International Conference on Indoor Positioning and Indoor Navigation (IPIN), Nuremberg, Germany, 25–28 September 2023; pp. 1–6. [CrossRef]

8. Rosiak, M.; Kawulok, M.; Maćkowski, M. The Effectiveness of UWB-Based Indoor Positioning Systems for the Navigation of Visually Impaired Individuals. *Appl. Sci.* **2024**, *14*, 5646. [CrossRef]
9. Warnakulasuriya, H.N.; Dorji, T.; Horanont, T. Indoor Positioning Based on Time of Flight and Kalman Filtering Using Ultra-Wideband Sensors. In Proceedings of the 2024 IEEE International Conference on Big Data and Smart Computing (BigComp), Bangkok, Thailand, 18–21 February 2024; pp. 117–123.
10. Drahanský, M.; Macek, I.; Goldmann, T. Monitoring of visitors in museum exhibitions. *J. Natl. Mus. (Prague) Nat. Hist. Ser.* **2020**, *189*, 155–162. [CrossRef]
11. Alarifi, A.; Al-Salman, A.; Alsaleh, M.; Alnafessah, A.; Al-Hadhrami, S.; Al-Ammar, M.A.; Al-Khalifa, H.S. Ultra wideband indoor positioning technologies: Analysis and recent advances. *Sensors* **2016**, *16*, 707. [CrossRef] [PubMed]
12. Deputter, M. Ultra-Wideband Versus Other Location Technologies. 2024. Available online: https://www.pozyx.io/newsroom/uwb-versus-other-technologies#uwb-vs-ble (accessed on 9 February 2025).
13. Penggang, G.; Gao, L.; Yunhui, L.; Wen, C. A Novel Method for UWB-based Localization Using Fewer Anchors in a Floor with Multiple Rooms and Corridors. In Proceedings of the 2022 IEEE 12th International Conference on Indoor Positioning and Indoor Navigation (IPIN), Beijing, China, 5–7 September 2022; pp. 1–6. [CrossRef]
14. Qiao, J.; Yang, F.; Liu, J.; Huang, G.; Zhang, W.; Li, M. Advancements in Indoor Precision Positioning: A Comprehensive Survey of UWB and Wi-Fi RTT Positioning Technologies. *Network* **2024**, *4*, 545–566. [CrossRef]
15. Sung, S.; Kim, H.; Jung, J.I. Accurate indoor positioning for UWB-based personal devices using deep learning. *IEEE Access* **2023**, *11*, 20095–20113. [CrossRef]
16. Di Pietra, V.; Dabove, P.; Piras, M. Loosely Coupled GNSS and UWB with INS Integration for Indoor/Outdoor Pedestrian Navigation. *Sensors* **2020**, *20*, 6292. [CrossRef] [PubMed]
17. D'Urso, P.R.; Arcidiacono, C.; Pastell, M.; Cascone, G. Assessment of a UWB Real Time Location System for Dairy Cows' Monitoring. *Sensors* **2023**, *23*, 4873. [CrossRef] [PubMed]
18. Gnaś, D.; Majerek, D.; Styła, M.; Adamkiewicz, P.; Skowron, S.; Sak-Skowron, M.; Ivashko, O.; Stokłosa, J.; Pietrzyk, R. Enhanced Indoor Positioning System Using Ultra-Wideband Technology and Machine Learning Algorithms for Energy-Efficient Warehouse Management. *Energies* **2024**, *17*, 4125. [CrossRef]
19. Yi, T.; Lee, J.H. The Process of Visitor Studies in Art Museum Tracking the Behavior of Museum Visitors. In Proceedings of the 2nd International Conference on Intelligent Human Systems Integration (IHSI), San Diego, CA, USA, 7–10 February 2019.
20. Dabove, P.; Di Pietra, V.; Piras, M.; Jabbar, A.A.; Kazim, S.A. Indoor positioning using Ultra-wide band (UWB) technologies: Positioning accuracies and sensors' performances. In Proceedings of the 2018 IEEE/ION Position, Location and Navigation Symposium (PLANS), Monterey, CA, USA, 23–26 April 2018; pp. 175–184.
21. Ge, L.; Deng, Z.; Liu, W.; Zhang, G.; Han, K.; Jiao, J. Wireless clock synchronization based on UWB positioning system and its ranging optimization. In Proceedings of the 2018 Ubiquitous Positioning, Indoor Navigation and Location-Based Services (UPINLBS), Wuhan, China, 22–23 March 2018; pp. 1–6. [CrossRef]
22. Blazek, J.; Jiranek, J.; Bajer, J. Indoor Passive Positioning Technique using Ultra Wide Band Modules. In Proceedings of the 2019 International Conference on Military Technologies (ICMT), Brno, Czech Republic, 30–31 May 2019; pp. 1–5. [CrossRef]
23. Fakhoury, S.; Ismail, K. Ultra-Wideband-Based Time Occupancy Analysis for Safety Studies. *Sensors* **2023**, *23*, 7551. [CrossRef] [PubMed]
24. Masiero, A.; Fissore, F.; Vettore, A. A Low Cost UWB Based Solution for Direct Georeferencing UAV Photogrammetry. *Remote Sens.* **2017**, *9*, 414. [CrossRef]
25. Tobii, A.B. Tobii Pro Glasses 3–Wearable Eye-Tracker. Available online: https://www.tobii.com/products/eye-trackers/wearables/tobii-pro-glasses-3 (accessed on 12 June 2025).
26. Silverstein, P.; Westermann, G.; Parise, E.; Twomey, K. New evidence for learning-based accounts of gaze following: Testing a robotic prediction. In Proceedings of the 2019 Joint IEEE 9th International Conference on Development and Learning and Epigenetic Robotics (ICDL-EpiRob), Oslo, Norway, 19–22 August 2019; pp. 302–306. [CrossRef]
27. Rudenko, S.; Danilina, N.; Hristov, B. Using a mobile eye-tracking technology to explore pedestrians' gaze distribution on street space. In *Proceedings of the E3S Web of Conferences*; EDP Sciences: Les Ulis, France, 2021; Volume 263, p. 5015. [CrossRef]
28. Makellaraki, A.; Di Pietra, V.; Dabove, P. Assessing Material Impacts in NLOS UWB Ranging Errors: Characterization for Museum Environments. In Proceedings of the 2025 IEEE/ION Position, Location and Navigation Symposium (PLANS), Salt Lake City, UT, USA, 28 April–1 May 2025.